

# We are IntechOpen, the world's leading publisher of Open Access books Built by scientists, for scientists

6,900

Open access books available

185,000

International authors and editors

200M

Downloads

Our authors are among the

154

Countries delivered to

TOP 1%

most cited scientists

12.2%

Contributors from top 500 universities



WEB OF SCIENCE™

Selection of our books indexed in the Book Citation Index  
in Web of Science™ Core Collection (BKCI)

Interested in publishing with us?  
Contact [book.department@intechopen.com](mailto:book.department@intechopen.com)

Numbers displayed above are based on latest data collected.  
For more information visit [www.intechopen.com](http://www.intechopen.com)



---

# Sputtered Hydroxyapatite Nanocoatings on Novel Titanium Alloys for Biomedical Applications

---

Kun Mediaswanti, Cuie Wen, Elena P. Ivanova,  
Christopher C. Berndt and James Wang

Additional information is available at the end of the chapter

<http://dx.doi.org/10.5772/54263>

---

## 1. Introduction

Titanium and titanium alloys have been extensively studied for many applications in the area of bone tissue engineering. It was believed that the excellent properties of titanium alloys, e.g. lightweight, excellent corrosion resistance, high mechanical strength and low elastic modulus compared to other metallic biomaterials such as stainless steels and Cr-Co alloys, would provide enhanced stability for load-bearing implants. However, they usually lack sufficient osseointegration for implant longevity, and their biocompatibility is also an important concern in these applications due to the potential adverse reactions of metallic ions with the surrounding tissues once these metallic ions are released from the implant surfaces. One approach for consideration to improve the healing process is the application of a hydroxyapatite nanocoating onto the surface of biomedical devices and implants. Hydroxyapatite, with its excellent biocompatibility, and similar chemistry and structure to the mineral component of bone, provides a bioactive surface for direct bone formation and apposition with adjacent hard tissues. The deposition of a SiO<sub>2</sub> interlayer between the implant surface and the hydroxyapatite nanocoating is necessary to further improve the biocompatibility of metal implants, as SiO<sub>2</sub> has its own excellent compatibility with living tissues, and high chemical inertness, which lead to enhanced osteointegrative and functional properties of the system as a whole.

Therefore, SiO<sub>2</sub> and hydroxyapatite nanocoatings were deposited onto titanium alloys using electron beam evaporation and magnetron sputtering techniques, respectively, with different process parameters to optimize the deposition conditions and so achieve desired properties. Surface characteristics are essential due to their role in enhancing osseointegration. Surface morphology and microstructure were observed using a scanning electron micro-

scope (SEM) and elemental analysis was performed by the energy dispersive X-ray spectroscopy method (EDS). The crystal structure was examined using X-ray diffractometer (XRD) to identify the phase components, while nanocoating thickness was measured using profilometer.

This chapter is divided into five major parts. First is an overview of bone and bone implants, including their structure and mechanical properties. The second part highlights the importance of nanocoatings for bone implants longevity. Various coatings and surface modification techniques of titanium and its alloys are also elucidated. The advantages and drawbacks of each technique are reviewed. The last part focuses on the study of sputtered hydroxyapatite and SiO<sub>2</sub> nanocoatings on titanium. A thorough discussion of the results is presented.

## 2. Natural bone and bone implants

### 2.1. Natural bone

Bone is a complex living tissue that harnesses the synergies of osseous tissue, cartilage, dense connective tissues, epithelium, adipose tissue and nervous tissue. Bone as a functional organ in the human body has various roles, such as supporting soft tissues, protecting many internal organs, enabling movements in human activity and facilitating mineral homeostasis, *i.e.*, storage of osseous tissue minerals such as calcium and phosphate, providing blood cell production sites and acting as a location for triglyceride storage [1].

Bone consists of both organic and inorganic materials that are distributed within an extracellular matrix. Organic material, called fibrous protein collagen, is predominant in bone structure and this collagen contributes to the tensile strength of bone. The inorganic material impregnated inside bone is mainly hydroxyapatite, *i.e.*, minerals of calcium phosphate and calcium carbonate. Usually, the calcium to phosphorus ratio of natural bone ranges between 1.50-1.65 depending on its location. Around 25 wt.% of bone consists of water that is present in bone pores, thereby ensuring nutrient diffusion and contributing to the viscoelastic properties of the material. Calcification is a process of crystallisation of mineral salts *i.e.*, calcium phosphate, which occurs in the biological framework formed by the collagen fibres [2].

There are four types of cells in osseous tissues: osteogenic cells, osteoblasts, osteocytes and osteoclasts. Osteogenic cells undergo cell division and develop into osteoblasts. Osteoblasts play a role in bone formation and collagen secretion. As osteoblasts secrete extracellular matrix, then osteoblasts evolve into osteocytes. Osteocytes, also known as mature bone cells, are responsible for nutrients and waste exchange with the blood. Osteoclasts are bone destroying cells and responsible for bone resorption. Bone consists of bone lining cells, fibroblasts, and fibrocytes. Bone lining cells control the movement of ions between bone and the surrounding tissue. The role of fibroblasts and fibrocytes is, in brief, to form collagen [1].

Bone can be categorized into five types on the basis of its shape, namely long, short, flat, irregular, and sesamoid. In addition to the dense structures present, osseous tissue has many

small spaces between its cellular and extracellular matrix. There are two types of osseous tissue on the basis of the size and distribution of these spaces: compact bone tissue and spongy bone tissue. About 80 wt.% of the human skeleton is compact bone tissue. Compact bone consists of a packed osteon within the Haversian architecture. Each osteon consists of a central Haversian canal, concentric lamellae, lacunae, osteocytes, and canaliculi. Spongy bone, also termed as trabecular bone, exhibits a porous structure with porosity ranging from 50-90 wt.% and consists of an integrate lamellae network. The role of trabeculae is to support and protect the red bone marrow [2].

Bone structure contains macro, micro and nanoscale pores with different functions and characteristics. Macro-scale porosity gives rise to mechanical anisotropy. Micro-scale porosity provides sufficient vascularisation and cell migration, while nanoscale features act as a framework for cell and mineral binding [2].

Bone mechanics is determined mainly by the bone structure. Compact bone is stiffer and stronger than cancellous bone. The mechanical properties of human bone are listed in Table 1 [2]. The elastic modulus of human bone is approximately 0.05-2 GPa for cancellous bone and 7-30 GPa for compact bone [2]. It should be kept in mind that “elastic modulus” is not an exact description for bone properties since they are anisotropic and viscoelastic.

| Mechanical Properties    | Human Haversian (MPa) |
|--------------------------|-----------------------|
| Tensile strength         | 158                   |
| Tensile yield stress     | 128                   |
| Compressive strength     | 213                   |
| Compressive yield stress | 180                   |
| Shear strength           | 71                    |

**Table 1.** Mechanical properties of human haversian [2]

## 2.2. Bone implant

The history of implants started with the applications of autograph, allograft, and artificial device techniques [3]. Autographs utilized tissues from other parts of the patient’s body, whilst allograft techniques used tissue from a donor. However, both techniques had drawbacks in application. The autograph method was limited only to nose bone and finger junctions [3]. Moreover, there were adverse side effects, such as infections and pain at the implant area. The allograft technique required a compatible donor that matched the patient’s body system, which was usually difficult to find. There was always the potential risk of infections and disease transmission from the donor to the recipient’s body. Artificial grafts employed artificial materials, now known as biomaterials. The advantages of using artificial device grafts include (i) lower risk for any transmission of disease, (ii) a reduced risk of infections, and (iii) the availability of many biomaterials for potential use as scaffolds. Therefore, ongoing studies aim to develop a new generation of biomaterials for bone implants.

### 2.3. Criteria of ideal bone implant

An ideal bone implant material should be osteoconductive, osteoinductive and should have osseointegration ability [3]. Furthermore, other key criteria for excellent implant performance include biocompatibility and mechanical compatibility. In addition, any implant waste after degradation should not cause harmful effects to the body. Recent trends in bone tissue engineering studies have revealed that bone implants may also serve as a drug delivery system if they are appropriately designed.

Osteoconduction is a process by which bone is directed to conform to a material's surface, while osteoinduction is the ability of an implant to induce osteogenesis. An inductive agent will stimulate undifferentiated cells to form preosteoblasts [3]. According to Branemark *et al.* [4], osseointegration could be defined as the "continuing structural and functional co-existence, possibly in a symbiotic manner, between differentiated, adequately remodelled, biologic tissues, and strictly defined and controlled synthetic components, providing lasting, specific clinical functions without initiating rejection mechanisms".

In the context of orthopaedic implants, the development of a drug delivery system is still at an early developing stage. The promising concept of using an implant as part of a drug delivery system could be described as the integration of therapeutic agents and devices.

In addition to high mechanical strength, the Young's modulus is a critical mechanical property in an artificial device when designing materials for bone implants. Other fundamental requirements for an ideal orthopaedic biomedical implant include high wear resistance, good fatigue properties if used under cyclic loading, no adverse tissue reactions, and high corrosion resistance.

## 3. Titanium and titanium alloys as bone implant materials

The applications of titanium in modern society, such as aviation and military defence, have been exploited widely. Titanium components have also been used in biomedical devices, including screws, plates, and hip and knee prostheses, for either bone fractures or bone replacement. These proven applications can be attributed to the distinctive properties of titanium and its alloys; properties such as high strength to density ratio and high corrosion resistance that enable their use as bone substitutes under load bearing conditions. Moreover, titanium exhibits a high tensile strength that is not featured in polymer or ceramic biomaterials. However, the long term inertness of titanium towards human tissues after implantation is a major drawback, as this means a lack of direct chemical bonding between the implant and host tissues [5-6].

Another concern regarding the use of solid titanium is that the dense structure is unable to support new bone tissues in growth and vascularisation. In addition, titanium has a much higher elastic modulus than natural bone, *i.e.*, 5 GPa and 110 GPa for bone and dense titanium, respectively [7-8]. This biomechanical mismatch causes stress shielding and, eventually, may lead to aseptic loosening that results in additional surgery after 10-15

years of implantation [9]. The development of porous titanium may potentially overcome problems of this nature.

The development of new titanium alloys has been extensively explored. Usually Al, Sn, O, C, N, Ga, and Zr are used as  $\alpha$  stabilizers, while V, Mo, Ta, Nb, and Cr are used as  $\beta$  stabilizers [10]. Titanium alloys such as Ti6Al4V with aluminium and vanadium as  $\alpha$  and  $\beta$  stabilizing elements have been widely used as implant materials. These first generation biomedical titanium alloys, however, have revealed that the release of Al and V metal ions is harmful to the human body [11]. The decisive requirement of a biomedical implant is its biocompatibility in the human body. Thus, alloying elements must be carefully chosen to reduce any biologically adverse impacts. Alloying elements that attract biomedical applications are Ta, Nb, and Zr due to their non-cytotoxicity, good biocompatibility, high corrosion resistance and their complete solid solubility in titanium [10].

Beta alloys that have higher  $\beta$  stabilizers content are attracting great interest for bone implant applications due to their low elastic modulus. Beta alloys that have been studied for bone implant applications include Ti50Ta20Zr, Ti64Ta, Ti13Nb13Zr, Ti42Nb, and Ti30Zr10Nb10Ta. Studies conducted by Obbard *et al.* [12] showed that by adjusting the concentration of  $\beta$  stabilizer Ta, the elastic modulus could be reduced. In this fashion the compliance mismatch between the implant and bone would be reduced, leading to lesser stress shielding.

Alpha-beta alloys may have some advantages over  $\beta$  alloys, namely lower density and higher tensile ductility. Some studies have succeeded in the production of alpha-beta alloys with a porous structure. The porous structure serves as an anchorage for bone in-growth and exhibits a lower elastic modulus, while the  $\alpha$  and  $\beta$  phases provide sufficient mechanical strength for load bearing applications.

The development of porous titanium alloys with a variety of alloy components has brought about many improvements in bio-mechanical properties. For example, porous Ti10Nb10Zr with 69% porosity exhibited a tensile strength of 67 MPa, while pure Ti and pure Ta scaffolds with the same porosity demonstrated lower strengths of 53 MPa and 35.2 MPa, respectively [13]. Xiong *et al.* [14] reported that the elastic moduli of porous Ti-26Nb alloys with porosity of 50, 60, 70, and 80% were 25.4, 11.0, 5.2 and 2.0 GPa, respectively, while the plateau strength ranged from 180 MPa to 11 MPa.

#### **4. The importance of nano-coatings for bone implant materials**

Surface modification is a process that changes the composition, microstructure and morphology of a surface layer while maintaining the mechanical properties of the material. The aim of surface modification is to improve the bioactivity of the biomaterials so that the biomaterials demonstrate a higher apatite inducing ability that, in turn, leads to rapid osseointegration. After surface treatment, it is expected that the implant's surface will form an active apatite layer. The role of the thin apatite layer is to be a bonding interface to stimulate

bone apatite and collagen production [15-16]. It is suggested that altering the nanostructured surface morphology influences the apatite inducing ability and improves osteoblast adhesion and differentiation [17].

#### 4.1. Calcium phosphate coatings

Calcium phosphate is a synthetic ceramic that has been proven to support bone apposition and to enhance the osteoconduction of the bone. Calcium phosphate ceramics for bone tissue applications include tricalcium phosphate (TCP), octocalcium phosphate (OCP), hydroxyapatite ( $\text{Ca}_{10}(\text{PO}_4)_6(\text{OH})_2$ , HA), and biphasic calcium phosphate (BCP) [18]. These ceramics accelerate the healing process and have been widely used in conjunction with metallic material as a bioactive coating material. The ratio of Ca/P in calcium phosphate should resemble the biological apatite mineral of bone (*i.e.*, 1.50-1.69). Calcium phosphate has the natural facility to bond directly to bone.

#### 4.2. Nano-hydroxyapatite coatings

Hydroxyapatite demonstrates the best bioactivity amongst all the forms of calcium phosphate. Hydroxyapatite (HA) exhibits functionality in promoting osteoblast adhesion, migration, differentiation and proliferation; all of which are essential for bone regeneration. HA also has the ability to bond directly onto bone. The bioactivity of HA has made this ceramic the favourite for implant applications. HA nanoparticles may also induce cancer cell apoptosis [19]. The crystalline form of HA exhibits biointegration and prevents formation of adverse fibrous tissue. It is a more desirable coating than amorphous HA due to its ability to provide a better substrate for a different cell line [20]. Amorphous HA tends to dissolve in human fluid more easily and leads to loosening of the implant. Nanocrystalline HA is more favourable than microcrystalline HA because of its structural similarity with apatite [21].

### 5. Surface modification techniques

#### 5.1. Sol-gel

The sol-gel method has been widely used to deposit calcium phosphate onto dense or porous metallic materials. There are two routes for a sol-gel reaction, namely inorganic and organic, using reagents consisting of a colloidal suspension solution of inorganic or organic precursors. The sol-gel technique transforms a liquid (sol) into a solid phase (gel) and requires drying and heat treatment stages. The advantages of the sol-gel method include: (i) it is cost-effective, (ii) it is easy to control the final chemical composition and thickness of the coating, (iii) the coating is readily anchored on the substrate, and it is usually homogenous with a good surface finish, and (iv) it can be used for coating implants or substrates that have complex surfaces or large surface areas.

Wen *et al.* [22] reported that a sol-gel method for HA and titania ( $\text{TiO}_2$ ) coatings exhibited excellent bioactivity after immersion in simulated body fluid (SBF) that mimics human body

fluid of a similar ion concentration and pH value to human blood plasma. In addition to enhancing titanium bioactivity, HA-titania coating is expected to increase the bonding strength and corrosion resistance. The surface morphology and microstructure of HA and titania coating before and after being immersed in SBF are presented in Figure 1 (a)-(d). It can be seen that the coating is dense, uniform and without cracks. Wen *et al.* also reported that after soaking in SBF, HA granules grow gradually.

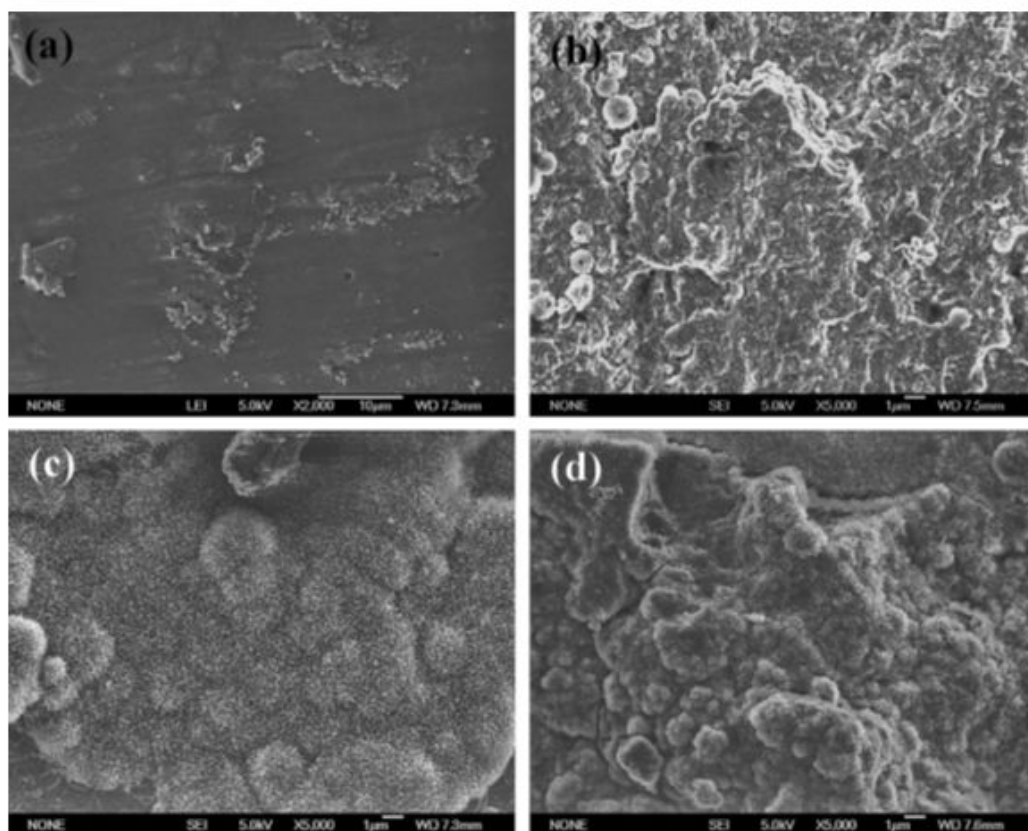


**Figure 1.** SEM micrographs of the surface morphology of HA/TiO<sub>2</sub> films after soaking in SBF for (a) 0 day, (b) 1 day, (c) 8 days, and (d) 15 days

## 5.2. Electrodeposition of materials

Electrodeposition is a coating method applied to the fabrication of computer chips and magnetic data storage. Recently, that has been rising interest in electrochemical deposition for tissue engineering applications due to its ability to coat complex 3D components.

Lopez-Heredia *et al.* [23] coated calcium phosphate onto porous titanium using the electrodeposition method. In the process, Ti, platinum mesh, and supersaturated calcium phosphate solution were used as the cathode, electrode and electrolyte, respectively. The ratio of Ca/P in the calcium phosphate coating was 1.65 and the coating thickness was 25 µm. The calcium phosphate coating was homogenous and covered the entire Ti surface. Moreover,

they reported that the coating presented good adhesion to the underlying substrate. The electrodeposition of CaP showed that calcium phosphate enhances the adherence of cells.

Adamek *et al.* [24] succeeded in producing an HA coating on porous Ti6Al4V using electrodeposition. The intermediate layer between the bone and metallic implant was rough and porous. Large pores and nanolamellae were present within the HA layer. The flexibility of the electrodeposition technique for coating solid and porous metallic implants has acquired increasing interest due to this ability to enhance the bioactivity of bone implant materials.

### 5.3. Biomimetic creation of surfaces

There are two major steps involved in the biomimetic technique. The first step is to conduct a pre-treatment of the implant material surface to create a layer functional group that can induce formation of an effective apatite layer. Several studies have revealed that an apatite layer has not been formed on materials without any treatment prior to immersion [25]. Preliminary treatment includes, for example, hydrothermal, sol-gel, alkali heat treatment and micro-arc. The second step is to immerse the biomaterials into a simulated body fluid (SBF). In this step, the bone apatite layer is formed on the biomaterial's surface. The high apatite forming ability of titanium arises from the formation of a hydrated titanate surface layer during chemical treatment. The advantages of the biomimetic process include (i) flexibility in the control of the chemical composition and thickness of the coating, (ii) the formation of relatively homogenous bioactive bonelike apatite coatings, (iii) a lower processing temperature, and (iv) the ability to coat 3D geometries.

Wang *et al.* [25] used a modified biomimetic approach to improve the biocompatibility of porous titanium alloy scaffolds. In their experiment, porous Ti10Nb10Zr underwent an alkali heat treatment prior to soaking in SBF. Two NaOH concentrations of 5 M and 0.5 M were used, and the samples were soaked for 1 week. The surface morphologies of porous TiNbZr after alkali soaking and heat treatment revealed a nanofiber layer, that consisted of sodium titanate. Parameters that influenced the morphology and thickness of the sodium titanate were reaction temperature and NaOH concentration.

Calcium phosphate was successfully deposited on the surface of the porous TiNbZr. The calcium phosphate layer was uniform and homogeneously spread onto the surface. Another biomimetic study, conducted by Habibovic *et al.* [26], indicated that a thick and homogenous crystalline hydroxyapatite coating was deposited on all pores and resembled bone minerals.

An evaporation-based biomimetic coating was introduced by Duan *et al.* [27]. In their study, a supersaturated calcium phosphate was prepared by mixing NaCl, CaCl<sub>2</sub>, HCl, NH<sub>4</sub>H<sub>2</sub>PO<sub>4</sub>, tri(hydroxymethyl)aminomethane (Tris), and distilled water, which they termed the accelerated calcification solution (ACS). Calcium phosphate crystallites formed on the surface on dipping the samples into the ACS. The main component in the coating was octa-calcium-phosphate (OCP) and apatite was observed after soaking in SBF. The advantages of this method include (i) no surface etching is required, (ii) high supersaturations of the coating chemistry can be achieved, and (iii) tight control of the solutions is achieved [27].

#### 5.4. Thermal spray

The thermal spray technique is a well-established and versatile technique that can be applied for a wide variety of coating materials, *i.e.*, metallic, non-metallic, ceramic, and polymeric. Thermal spray coated medical implants, such as orthopaedic and dental prostheses, have been commercially used. Thermal spray offers several advantages, such as the ability to coat low and high melting materials, a high deposition rate, and flexibility in coating 3D shape components. It is also cost effective [28]. Despite these advantages, some problems have been revealed after long term implantations using thermal spray coatings, such as delamination, resorption, biodegradation of the thick coating and mechanical instability [29]. Thus, improving the adhesion strength of thermal sprayed coatings is a major concern for bone or dental applications.

There are several types of thermal spraying; for example, plasma spray, flame spray, and cold spray [29]. Plasma spray is commonly applied to produce thick coatings for metallic corrosion protection. It is also flexible, due to its ability to coat different substrates. During plasma spraying, the precursor is atomised and injected into plasma jet, then accelerated towards the substrate with the aid of an inert carrier gas [30]. There are many parameters that must be controlled to produce a high quality coating.

Flame spray uses a combustion flame to melt the solid precursor. There is, additionally, another type of flame spray termed as high velocity oxygen fuel (HVOF). This technology is favourable due to its high spray velocity and the formation of a strong bond coating [30-32].

The thermal spray technique has been widely employed for HA coatings. The surface morphology of HA coatings obtained with various parameters of stand-off distance (SOD) and power are presented in Figure 2 (a)-(d). Sun *et al.* [28] reported that when the spray power increased, the crystallinity of HA decreased and the amorphous phase became more obvious. The effect of SOD indicated an inverse correlation with deposition efficiency. Several parameters that influence the deposition of HA are SOD, spray power, feedstock particle size and velocity.

Cold spray is a new member of the thermal spray family. This technique uses small particles of 1-50  $\mu\text{m}$ . A supersonic jet of compressed gas is used to accelerate the particles. The advantage of using this technique is the ability to produce dense coatings and maintain the material chemistry and phase composition of the feedstock. Noppakun *et al.* [33] have applied cold spray technique to deposit HA-Ag/poly-ester-ether-ketone on glass slides. This study reported that cold spray was able to retain and elicit a coating functionality that was the same as the starting materials.

#### 5.5. Physical vapor deposition

Physical vapor deposition (PVD) is a deposition method where materials are evaporated or sputtered, transferred and deposited onto the substrate surface. This physical process includes thermal evaporation or plasma-induced ion bombardment onto the sputtering target. A condensation or reaction of the coating materials then takes place on the substrate surface to form coatings. Variants of the PVD process include evaporation, ion plating, pulsed laser dep-

osition and sputtering. The beneficial features of PVD are high coating density, high bio-adhesion strength, formation of multi-component layers, and low substrate temperature [34].

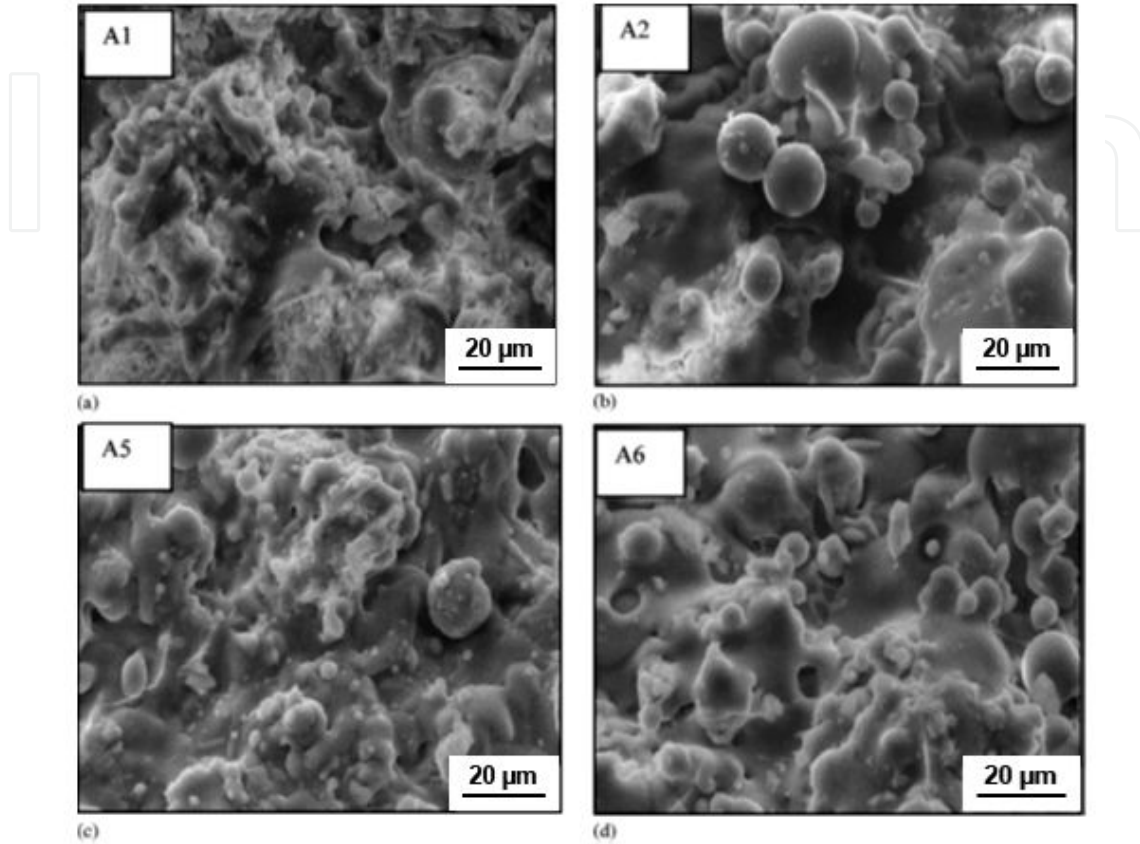


**Figure 2.** Surface morphology of HA coatings obtained by thermal spray method (a) 27.5 kW at 80 mm SOD, (b) 27.5 kW at 160 mm SOD, (c) 42 kW at 80 mm SOD, and (d) 42 kW at 160 mm SOD

Evaporation involves the thermal phase change from solid to vapor under vacuum conditions, in which evaporated atoms of a solid precursor placed in an open crucible can travel directly and condense onto the surface of a substrate [35]. A vacuum environment is used to minimize contamination [36]. Han *et al.* [37] have created an HA coating using electron beam evaporation and then incorporated silver by immersion into  $\text{AgNO}_3$  solution. One advantage of this method is an improved bond strength between the coating and substrate. The ratio of Ca/P in the HA coating was 1.62 with a bond strength of 64.8 MPa, which was significantly higher than a plasma sprayed bond strength of 5.3 MPa [37].

Sputtering involves a process of ejecting neutral atoms from a target surface using energetic particle bombardment. The energetic particles used in the sputtering process are argon ions, which can be easily accelerated towards the cathode by means of an applied electric potential, hence bombarding the target, and ejecting neutral atoms from the target. These ejected atoms are then transferred and condense to the substrate to form a coating. Sputtering has been used in many applications such as the semiconductor, photovoltaic and automotive

sectors. There are several sputtering methods, such as DC glow discharge, radio frequency (RF), ion beam sputtering (IBS), and reactive sputtering [36].

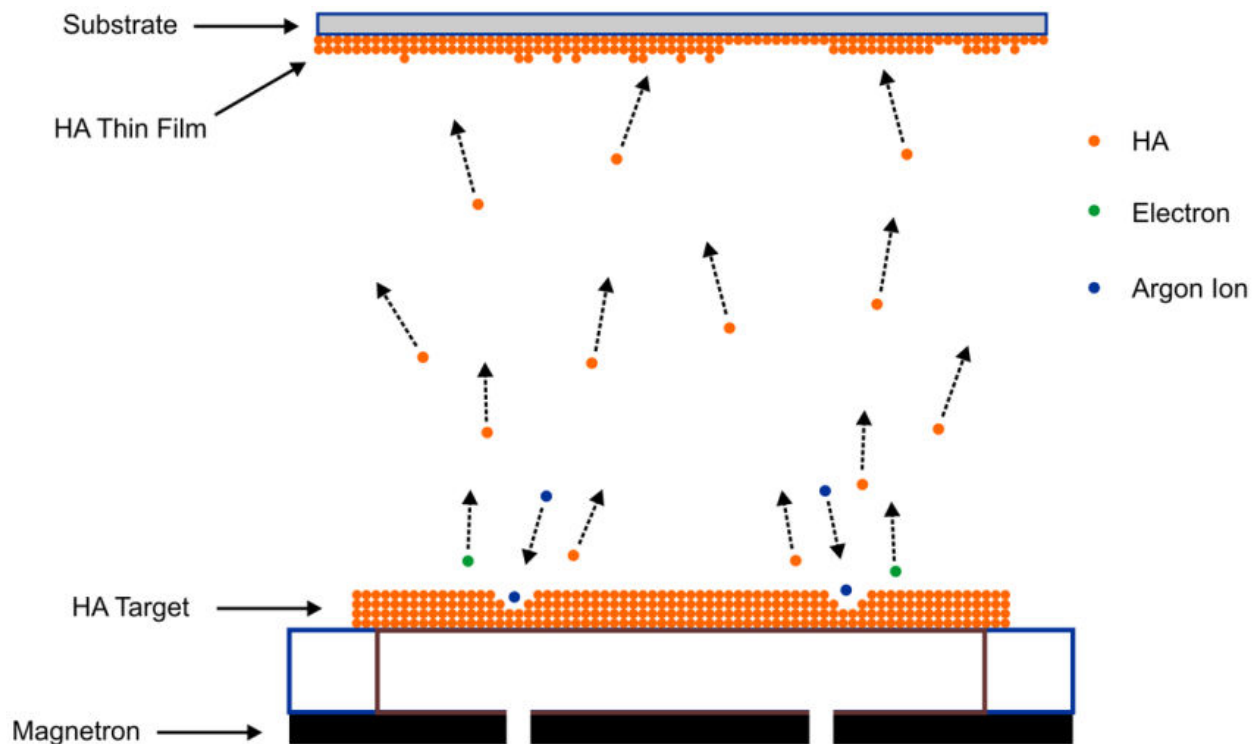


**Figure 3.** Schematic diagram of the sputtering mechanism

The simplest model for sputtering is the diode plasma, which consists of a pair of planar electrodes, an anode and a cathode, inside a vacuum system [37]. The sputtering target is mounted on the cathode. Application of the appropriate potential difference between the cathode and anode will ionize argon gas and create a plasma discharge. The argon ions will then be attracted and accelerated toward the sputtering target. Such ion bombardment on the target will displace some of the target atoms. This results in electron emission that will subsequently collide with gas atoms to form more ions that sustain the discharge [37]. Ion beam sputtering has disadvantages, such as a high capital investment cost (approximately one million dollars per machine), low deposition rates and a relatively small capacity per chamber batch [38]. Another type of sputtering employs radio frequency (RF) diodes that operate at high frequency.

Magnetron sputtering is one option to overcome the problems such as delamination and low bond strength that may arise with plasma spray methods. Magnetron sputtering enables lower pressures to be used, because a magnetic field allows trapping of the secondary electrons near the target. This induces more collisions with neutral gases and increases plasma ionisation. Figure 3 is a diagram of the magnetron sputtering mechanism. RF magnetron sputtering is an improved ion-sputtering method. It has also been noted that sputtered films possess higher adhesion to the substrate compared to the evaporation method.

A summary of the characteristics of the various coating techniques for calcium phosphate is presented in Table 2. Each technique has its own benefits and drawbacks. However, sputtering is a promising method due to its ability to produce dense and thin coatings, as well as provide good bond strength [39-41].

| Techniques        | Advantages  | Disadvantages   | Coating thickness      |
|-------------------|---|---|------------------------|
| Sol-gel           | Flexible in coating complex shapes,   | Sometimes expensive   | < 1 $\mu\text{m}$      |
| Electrodeposition | Flexible in coating complex shapes. Low energy process, can be scaled down to deposition of a few atoms or scaled up to large dimensions. | Tends to crack  | 25 $\mu\text{m}$       |
| Plasma Spray      | Able to coat high and low melting materials. High deposition rate   | Delamination and resorption. High temperature leads to decomposition                  | 50 - 100 $\mu\text{m}$ |
| Biomimetic        | Flexible in coating complex shapes and flexible in controlling chemical composition of the coating. Homogenous.                           | The use of alkali heat treatment could reduce mechanical strength. Requires much time | 10 - 30 $\mu\text{m}$  |
| Sputtering        | Dense, homogenous coating. Excellent adhesion   | Needs annealing for crystalline structure   | < 1 $\mu\text{m}$      |

**Table 2.** Summary of various techniques for calcium phosphate coatings

### 5.5.1. Properties of sputtered hydroxyapatite coatings

*Coating thickness.* The HA coating thickness varies. Molagic [42] succeeded in producing HA/ZrO<sub>2</sub> coatings with an average thickness of 3.2  $\mu\text{m}$ . Hong *et al.* [43] manufactured a 500 nm thick coating of crystalline HA using magnetron sputtering. Ding [44] sputter deposited HA/Ti coatings with a film thickness of 3-7  $\mu\text{m}$  onto a titanium substrate. Thian *et al.* [45] succeeded in incorporating silicon in hydroxyapatite (Si-HA) using magnetron sputtering and discovered its potential use as a bio-coating. The Si-HA film thickness was up to 700 nm.

*Bond strength.* An *in vitro* and *in vivo* experiment on coatings using the sputtering technique revealed coating detachment problems. Cooley *et al.* [46] reported that HA coatings were removed after 3 weeks of implantation. A bond layer coating was suggested to overcome this weak adhesion at the interface and subsequent delamination. Ievlev *et al.* [47] measured the adhesion strength of HA coatings with a sublayer and revealed that the adhesion strength

was higher than coatings without a sublayer. Nieh *et al.* [48] used titanium as a pre-coat on Ti6Al4V and found strong bonding between the Ti layer and the HA coating.

Layered materials have previously been demonstrated to improve bonding between dissimilar materials. According to Ding [45], the top layer provides an excellent interaction with the surrounding tissue and promotes bone healing. A functionally graded coating (FGC) is an alternative method to enhance coating adhesion strength. Ozeki *et al.* [49] prepared an FGC of HA/Ti onto a metallic substrate. The coating thickness was 1  $\mu\text{m}$  and consisted of 5 layers. The configuration of FGC was designed so that the HA was more dense near the surface, whilst the Ti was more dense near the substrate. The bonding strength using the FGC configuration was higher than using only HA, *i.e.*, 15.2 MPa and 8 MPa for the FGC and pure HA, respectively.

*Elastic properties.* Snyders *et al.* [50] manufactured HA via RF sputtering and revealed that the chemical composition influenced the elastic properties. As the Ca/P ratio decreased, the elastic modulus also decreased due to the insertion of Ca vacancies in the HA lattices.

### 5.5.2. Biological performance of sputtered hydroxyapatite coatings

The biological behaviour of biomaterials has been a fundamental criterion for successful candidate implant materials, along with their mechanical properties. The surface properties of a biomaterial play a significant role in the cell response. Thus, surface modification is an established strategy that has been used for biomedical applications due to its ability to enhance bioactivity. High cell density enhances bone formation. The cell adhesion behaviour and proliferation are influenced by several factors, such as pore size, porosity, and surface composition [51].

Thian *et al.* [45] carried out an *in vitro* test using a human osteoblast (HOB) cell model for a silicon incorporated hydroxyapatite (Si-HA) coating on titanium. The sample demonstrated an increase in metabolic activity compared to mono-HA coatings. Sputtered HA and Si coatings exhibited good differentiation of osteogenic cells and good biocompatibility. It was noted that the biological response was influenced by the crystallinity of the HA coatings. Sputtered composite coatings of HA with other compounds may provide additional advantages for implant performance. For instance, Chen *et al.* [52] incorporated silver into HA, conducted a cytotoxic and antibacterial test, and reported that the silver had an antibacterial effect since the bacterial attachment was reduced compared to coatings that did not contain silver.

## 6. Experimental methods

### 6.1. Design and preparation of titanium alloys

Tin and niobium were chosen as alloying elements because both metals are biocompatible and non-cytotoxic. The titanium alloy composition was designed using the molecular orbital DV-X $\alpha$  method [53]. The calculation of the nominal composition of the alloys was based on

two parameters, known as the bond order (Bo) and d-orbital energy level (Md). The parameter Bo is the covalent bond strength between titanium and an alloying element, while the parameter Md represents the d-orbital energy level of a transition alloying metal that correlates with the electro-negativity and the atomic radius of element. The list of Md and Bo values for each alloying elements (Ti, Nb and Sn) was obtained from a study conducted by Abdel Hady *et al.* [54].

Titanium alloys were fabricated using the powder metallurgy technique. Titanium powders (purity 99.7%), tin powders (purity 99.0%) and niobium powders (purity 99.8%) with particle sizes less than 45  $\mu\text{m}$  were used. Each component was first weighted to give the desired composition of Ti<sub>14</sub>Nb<sub>4</sub>Sn. Ammonium hydrogen carbonate ( $\text{NH}_4\text{HCO}_3$ ) was used as a space holder material. The particle size chosen was 300-500  $\mu\text{m}$  in diameter.

The desired porosity and pore size were controlled by adjusting the initial weight ratio of  $\text{NH}_4\text{HCO}_3$  to metal powders and the particle size of  $\text{NH}_4\text{HCO}_3$ . These components were mixed and blended in a planetary ball milling for 4 h with a weight ratio of ball to powder of 1:2 and a rotation rate of 100 rpm. A small amount of ethanol was employed during the mixing of the ammonium hydrogen carbonate with elemental metal powders to prevent segregation. After mixing the ammonium hydrogen carbonate with the metal powders, the mixture was pressed into green compacts in a 50 ton hydraulic press.

The green compacts were sintered at a pressure of  $1.3 \times 10^{-3}$  Pa using a vacuum furnace. Two steps of heat treatment were employed to produce porous structures. The first step was to burn out the space holder particles at 200°C for 2 h. The second step was to sinter the compacts at 1200°C for 10 h. Dense samples were prepared using powder metallurgy with the absence of space holder particles, and heat treatment was carried out at 1200°C. The dimensions of dense and porous titanium alloy samples were 9 mm in diameter and 2 mm in thickness for subsequent sample characterization. The sintering process was conducted at 1200°C for 10 h. A schematic diagram of the fabrication sequence for titanium alloys is presented in Figure 4.

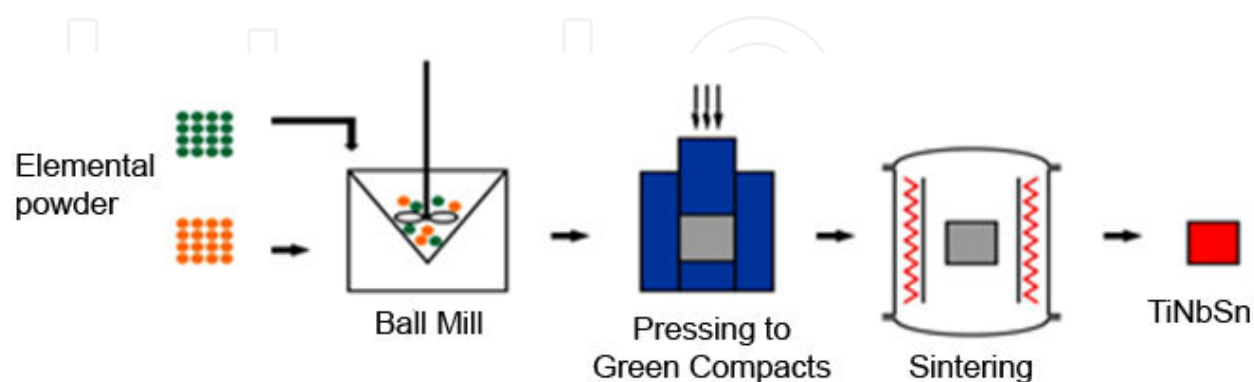


**Figure 4.** Schematic of Ti<sub>14</sub>Nb<sub>4</sub>Sn fabrication process by powder metallurgy route

Titanium alloy discs with 6 mm in diameter and 2 mm in thickness were gently wet ground-  
ed using (i) silicon carbide paper of 600 grit, (ii) followed by 1200 grit, and (iii) fine polished

using 15, 9, 6, and 1  $\mu\text{m}$  diamond compounds progressively. All metallic discs were then ultrasonically cleaned using ethanol for 5 min.

## 6.2. E-beam evaporation and sputtering

Silica thin films and nanocrystalline hydroxyapatite coatings were successively deposited onto the prepared titanium alloy substrates by e-beam evaporation and sputtering techniques. A HV thin film deposition system (CMS-18 Kurt J. Lesker, USA) was used. Both the e-beam evaporation and the sputtering processes were performed at room temperature. The base pressure of the system was  $6.6 \times 10^{-6}$  Pa.

A 200 nm  $\text{SiO}_2$  thin film was deposited at a working pressure of  $6.6 \times 10^{-4}$  Pa and a deposition rate of 10 nm/s. During the sputtering process, the working pressure was set at 0.8 Pa. The sputtering power was 90 W. The distance between the substrate and sputtering target was kept at 30 cm. During deposition, the substrate holder rotated in order to achieve uniform coating. Heat treatment of samples was performed at  $500^\circ\text{C}$  for 2 h in a vacuum furnace.

## 6.3. Characterization

The elemental composition was analyzed using an energy dispersive X-ray spectrometer (EDS, Oxford instruments INCA suite v.4.13) interfaced with a field-emission scanning electron microscope (FE-SEM, ZEISS SUPRA 40 VP) operated at 15 kV. Surface morphology of the samples was observed using scanning electron microscopy, and phase identification was performed using the X-ray diffraction method (XRD, Bruker D8 Advance), operated with  $\text{CuK}_\alpha$  radiation in the Bragg-Brentano mode at a scanning rate of  $0.5^\circ/\text{min}$  over a  $2\theta$  range of  $30\text{--}80^\circ$ . Phase analysis was conducted using the database PDF-2 version 2005.

The porosity of the scaffold was characterised by gravimetry using the formula [13]:

$$\varepsilon = \left(1 - \frac{\rho}{\rho_s}\right) \times 100 \quad (1)$$

where  $\rho$  and  $\rho_s$  are the actual and theoretical densities of the porous alloy, respectively.

## 7. Results and discussion

### 7.1. Physico-chemical properties of the Ti14Nb4Sn alloy

The X-ray diffraction pattern of sintered Ti14Nb4Sn is shown in Figure 5. Alpha peaks were observed at  $39.0^\circ$  and  $40.5^\circ$ , which are indexed as the reflection planes (101) and (103), while  $\beta$  peaks were observed at  $38.5^\circ$ , which is indexed as (110). The titanium alloy consisted of both  $\alpha$  and  $\beta$  phases. Weak niobium peaks were also detected, while tin was not detected. Elemental analysis using EDS was performed concurrently with the SEM examination to

identify the chemical composition of the samples. The EDS analyses verified that the alloy composition corresponded to Ti14Nb4Sn.

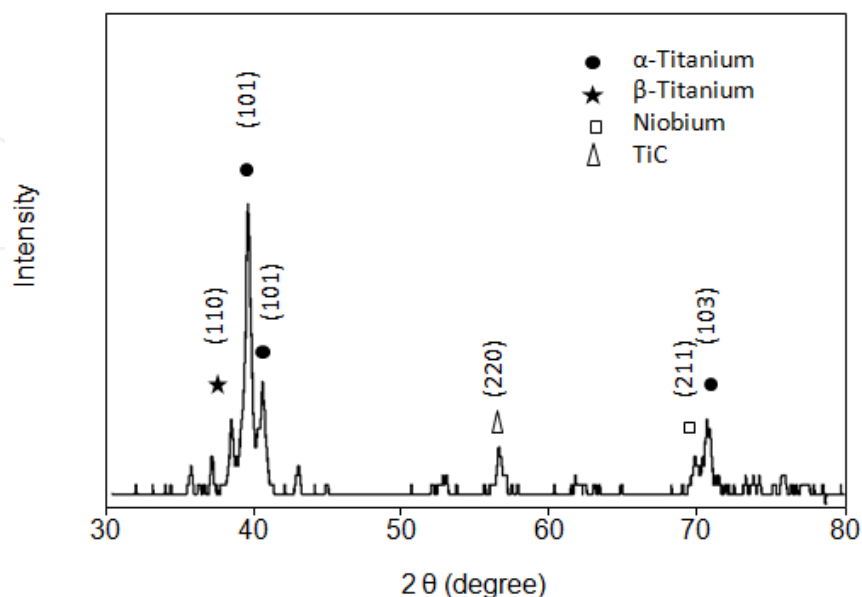


**Figure 5.** XRD pattern of sintered Ti14Nb4Sn alloy

SEM images of fabricated porous titanium alloys showed a combination of both macropores and micropores on the surface, as shown in Figure 6 (a)-(f). The micropore size ranged from 0.5 to 10  $\mu\text{m}$ , while the macropore size ranged from 50 to 700  $\mu\text{m}$ . Samples with greater porosity exhibited more interconnected features, more accessible inner surfaces, and interpenetrated macropores. It is believed that the optimal pore size to ensure vascularization and bone in-growth is 50-400  $\mu\text{m}$  [13]. Compared to other studies, fabrication of Ti10Nb10Zr alloy resulted in pore sizes ranging from 300 to 800  $\mu\text{m}$  since the size of the space-holder particles was set to be 500-800  $\mu\text{m}$  [13].

Usually there are two types of pores when using the space-holder method to fabricate titanium alloys: (i) macro-pores determined by the size of the space holder particles, and (ii) micro-pores determined by the dimension of the titanium powder particles. The micropores can be designed to allow the scaffold to be impregnated with functional coatings or therapeutic agents.

Porosity enhances the interlocking processes for the stability and immobility of the new implant, often referred to as stabilization and fixation of the implant. The porosity is influenced by several factors, namely the particle size of the metallic powder and the sintering pressure [13]. The porosity of the samples ranges from 55 to 80%. The optimum porosity of the implant for bone in-growth is in the range of 50-90%. It has been noted that the porosity level of an implant should be selected to provide the optimum mechanical behaviour, since porosity has a dominant and adverse influence on the strength of a porous material.

The pore connectivity, which can be determined by percolation theory, is a crucial parameter that determines successful bone in-growth. Connectivity between the pore provides sufficient area for physiological fluid to flow throughout the new tissue that enhances nutrient transportation. The images in Figure 6 exhibit variation in pores connectivity. High porosity results in high pore interconnectivity, *i.e.*, samples with 80% porosity exhibit high pore connectivity.

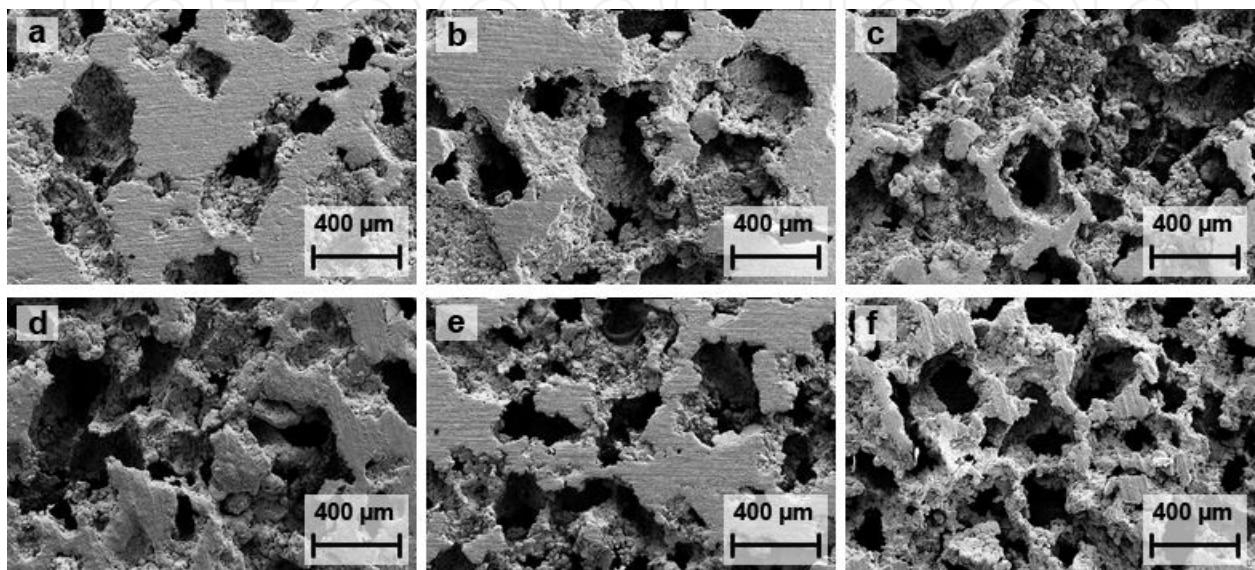
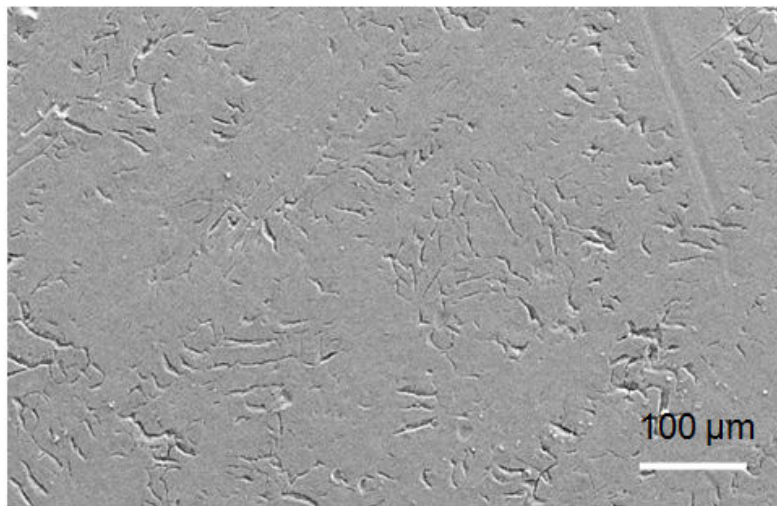


**Figure 6.** Morphology of porous Ti14Nb4Sn alloys with different porosity: (a) 55%, (b) 60%, (c) 70%, (d) 72%, (e) 75%, and (f) 80%

## 7.2. Physico-chemical properties of sputtered hydroxyapatite coated titanium alloys

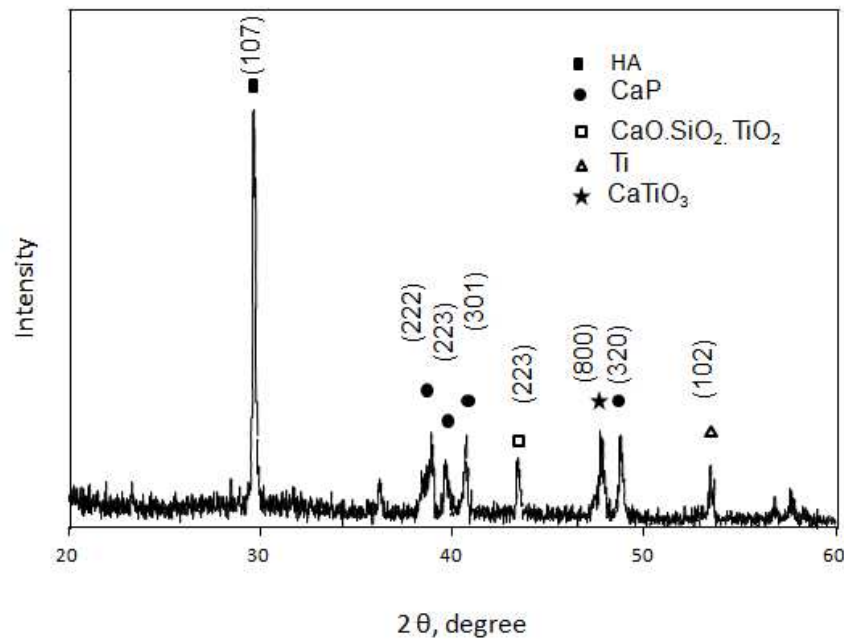
The application of SiO<sub>2</sub> as a bond layer between the substrate and the coating should improve coating adhesion to the substrate. One advantage of using silica is its influence on the bone mineralization process. Li *et al.* applied silica onto a titanium surface using a sol gel process and demonstrated its bioactivity [11]. Hong *et al.* [4] conducted an *in vitro* bioactivity test on bioactive ceramic glass with higher silicon content and revealed a superior mineralization capability. Thian *et al.* [46] succeeded in incorporating silicon into hydroxyapatite (Si-HA) using magnetron sputtering, and reported that higher silica content was beneficial for biomedical applications due to its higher corrosion resistance.

Figure 7 shows the surface topography of the HA-silica coating on titanium alloy Ti14Nb4Sn. The 2 μm thick hydroxyapatite coating and 200 nm thick SiO<sub>2</sub> film were deposited onto the titanium alloy using RF magnetron sputtering and e-beam evaporation, respectively. The HA coating was homogenous, which is characteristic of thin films deposited by sputtering. However, some cracks on the surface were observed. Some morphological features of rough coatings with some cracks could be advantageous for bone implant applications since this morphology could act as an anchorage for tissue growth.



**Figure 7.** Morphology of HA-SiO<sub>2</sub> coated Ti14Nb4Sn alloy

The XRD pattern of the HA-SiO<sub>2</sub> coated titanium alloys is shown in Figure 8. The identified phases were hydroxyapatite, CaO.SiO<sub>2</sub>.TiO<sub>2</sub>, calcium pyrophosphate, CaTiO<sub>3</sub> and titanium. After annealing, the crystalline phase of HA was present at  $2\theta = 30^\circ$  which matches the (107) plane. A peak corresponding to CaO.SiO<sub>2</sub>.TiO<sub>2</sub> phase was also observed at  $43.5^\circ$  and indexed as (223). In addition, the peak confirms the presence of the silica phase. The phase CaO, *i.e.*, in CaO.SiO<sub>2</sub>.TiO<sub>2</sub> observed in the XRD pattern could be related to the partial decomposition of hydroxyapatite during the deposition process.



**Figure 8.** XRD patterns of HA-SiO<sub>2</sub> coatings on Ti14Nb4Sn alloy

The titanium alloys are likely to be oxidized during the annealing process. Therefore,  $\text{TiO}_2$  appeared in the  $\text{CaO}\cdot\text{SiO}_2\cdot\text{TiO}_2$  phase and  $\text{CaTiO}_3$  phase. The  $\text{CaTiO}_3$  peak was detected at  $47.8^\circ$  with an orientation of (800). The four peaks at  $38.8^\circ$ ,  $39.7^\circ$ ,  $40.5^\circ$  and  $48.9^\circ$  corresponding to calcium phosphate ( $\text{Ca}_2\text{P}_2\text{O}_7$ ) are indexed as the reflection planes (222), (223), (301) and (320), respectively. However this phase might have higher solubility compared to HA. It is possible that during the sputtering process not all components of the HA target were sputtered and transferred onto the substrate. The titanium peak was present at  $53.5^\circ$  and indexed as (102). The results indicated that HA coatings using magnetron sputtering could produce the crystalline apatite phase.

## 8. Conclusions

This chapter describes the importance of developing a bioactive titanium alloy scaffold for bone tissue engineering applications. Ti14Nb4Sn alloy was designed and then fabricated using powder metallurgy method. The porosity ranged from 55 to 80% with pore sizes of 100-600  $\mu\text{m}$ .

Powder metallurgy that employed the space-holder sintering method was successful in fabricating samples for biomedical implant studies. The method produced porous structures that (i) enable better fixation, (ii) lower elastic modulus to match the properties of natural bone, and (iii) construct morphologies that mimic the features of natural bone structures.

To further enhance the biocompatibility of titanium alloys, 2  $\mu\text{m}$  thick hydroxyapatite and 200 nm thick  $\text{SiO}_2$  coatings were deposited onto Ti alloys using e-beam evaporation and RF magnetron sputtering. SEM images showed that the microstructure of the hydroxyapatite coating is homogenous, with some cracks appearing on its surface. XRD results confirmed that the coatings consisted of an HA phase with some  $\text{CaO}\cdot\text{SiO}_2\cdot\text{TiO}_2$ ,  $\text{CaTiO}_3$  and phases. Silica was also present in the XRD spectrum, which corresponds to the  $\text{CaO}\cdot\text{SiO}_2\cdot\text{TiO}_2$  phase. It was demonstrated that the e-beam evaporation and magnetron sputtering methods are suitable for depositing silica and hydroxyapatite coatings. The hydroxyapatite-silica configuration may be useful for biomedical implants, as it provides better adhesion strength for rapid osseointegration acceleration. Further study will focus on the biological response of these coatings.

## Acknowledgements

CW acknowledges the financial support from the Australian Research Council (ARC) through the ARC Discovery Project DP110101974.

## Author details

Kun Mediaswanti<sup>1</sup>, Cuie Wen<sup>1</sup>, Elena P. Ivanova<sup>2</sup>, Christopher C. Berndt<sup>1,3</sup> and James Wang<sup>1\*</sup>

\*Address all correspondence to: jawang@swin.edu.au

1 Industrial Research Institute Swinburne, Faculty of Engineering and Industrial Sciences, Swinburne University of Technology, Hawthorn, Australia

2 Faculty of Life and Social Sciences, Swinburne University of Technology, Hawthorn, Australia

3 Adjunct Professor, Materials Science and Engineering, Stony Brook University, Stony Brook, New York, USA

## References

- [1] Jenkins GW, Kemnitz CP, Tortora GJ. *Anatomy and Physiology from Science to Life*. New Jersey: John Wiley & Sons, Inc.; 2007.
- [2] Currey JD. *Bones: Structure and Mechanics*. New Jersey: Princeton University Press; 2002.
- [3] Bauer T, Muschler G. Bone graft materials. An overview of the basic science. *Clinical Orthopaedic Related Research* 2000;371:10-27.
- [4] Brånemark R, Brånemark PI, Rydevik B, Myers RR. Osseointegration in skeletal reconstruction and rehabilitation: a review. *Journal of Rehabilitation Research and Development*. 2001;38(2):175-81.
- [5] Jafari SM, Bender B, Coyle C, Parvizi J, Sharkey PF, Hozack WJ. Do tantalum and titanium cups show similar results in revision hip arthroplasty? *Clinical Orthopaedics and Related Research*. 2010;468(2):459-65.
- [6] Long M, Rack HJ. Titanium alloys in total joint replacement - A materials science perspective. *Biomaterials*. 1998;19(18):1621-39.
- [7] Kujala S, Ryhanen J, Danilov A, Tuukkanen J. Effect of porosity on the osteointegration and bone ingrowth of a weight-bearing nickel–titanium bone graft substitute. *Biomaterials*. 2003;24:4691–7.
- [8] LeGeros RZ, Craig RG. Strategies to affect bone remodeling: Osteointegration. *Journal of Bone and Mineral Research*. 1993;8(Suppl. 2):S583-S96.
- [9] Hollister SJ. Porous scaffold design for tissue engineering. *Nature Materials*. 2005;4(7):518-24.

- [10] Li Y, Wong C, Xiong J, Hodgson P, Wen C. Cytotoxicity of titanium and titanium alloying elements. *Journal of Dental Research*. 2010;89(5):493-7.
- [11] Okazaki Y, Rao S, Asao S, Tateishi T, Katsuda SI, Furuki Y. Effects of Ti, Al and V concentrations on cell viability. *Materials Transactions, JIM*. 1998;39(10):1053-62.
- [12] Obbard EG, Hao YL, Akahori T, Talling RJ, Niinomi M, Dye D, et al. Mechanics of superelasticity in Ti-30Nb-(8-10)Ta-5Zr alloy. *Acta Materialia*. 2010;58(10):3557-67.
- [13] Wang XJ, Li YC, Xiong JY, Hodgson PD, Wen CE. Porous TiNbZr alloy scaffolds for biomedical applications. *Acta Biomaterialia*. 2009;5(9):3616-24.
- [14] Xiong JY, Li YC, Hodgson PD, Wen CE. Mechanical properties of porous Ti-26Nb alloy for regenerative medicine. Fan JH, Chen HB. *Advances in Heterogeneous Material Mechanics*. 2008: 630-634.
- [15] Chen X, Nouri A, Li Y, Lin J, Hodgson PD, Wen C. Effect of surface roughness of Ti, Zr, and TiZr on apatite precipitation from simulated body fluid. *Biotechnology and Bioengineering*. 2008;101(2):378-87.
- [16] Kokubo T. Bioactive glass ceramics: properties and applications. *Biomaterials*. 1991;12(2):155-63.
- [17] Li J, Habibovic P, Yuan H, van den Doel M, Wilson CE, de Wijn JR, et al. Biological performance in goats of a porous titanium alloy-biphasic calcium phosphate composite. *Biomaterials*. 2007;28(29):4209-18.
- [18] Suzuki Y, Nomura N, Hanada S, Kamakura S, Anada T, Fuji T, et al. Osteoconductivity of porous titanium having young's modulus similar to bone and surface modification by OCP. *Key Engineering Materials*. 2007;330-332(II): 951-4.
- [19] Hu S, Li S, Yan Y, Wang Y, Cao X. Apoptosis of cancer cells induced by HAP nanoparticles. *Journal Wuhan University of Technology, Materials Science Edition*. 2005;20(4):13-5.
- [20] Hu Q, Tan Z, Liu Y, Tao J, Cai Y, Zhang M, et al. Effect of crystallinity of calcium phosphate nanoparticles on adhesion, proliferation, and differentiation of bone marrow mesenchymal stem cells. *Journal of Materials Chemistry*. 2007;17(44):4690-8.
- [21] Dumbleton J, Manley MT. Hydroxyapatite-coated prostheses in total hip and knee arthroplasty. *Journal of Bone and Joint Surgery - Series A*. 2004;86(11):2526-40.
- [22] Wen CE, Xu W, Hu WY, Hodgson PD. Hydroxyapatite/titania sol-gel coatings on titanium-zirconium alloy for biomedical applications. *Acta Biomaterialia*. 2007;3(3): 403-10.
- [23] Lopez-Heredia MA, Sohier J, Gaillard C, Quillard S, Dorget M, Layrolle P. Rapid prototyped porous titanium coated with calcium phosphate as a scaffold for bone tissue engineering. *Biomaterials*. 2008;29(17):2608-15.

- [24] Adamek G, Jakubowicz J. Mechanoelectrochemical synthesis and properties of porous nano-Ti-6Al-4V alloy with hydroxyapatite layer for biomedical applications. *Electrochemistry Communications*. 2010;12(5):653-6.
- [25] Wang X, Li Y, Hodgson PD, Wen C. Biomimetic modification of porous TiNbZr alloy scaffold for bone tissue engineering. *Tissue Engineering - Part A*. 2010;16(1):309-16.
- [26] Habibovic P, Barrère F, Van Blitterswijk CA, De Groot K, Layrolle P. Biomimetic hydroxyapatite coating on metal implants. *Journal of the American Ceramic Society*. 2002;85(3):517-22.
- [27] Duan K, Tang A, Wang RZ. A new evaporation-based method for the preparation of biomimetic calcium phosphate coatings on metals. *Materials Science & Engineering C-Biomimetic and Supramolecular Systems*. 2009;29(4):1334-7.
- [28] Sun L, Berndt CC, Grey CP. Phase, structural and microstructural investigations of plasma sprayed hydroxyapatite coatings. *Materials Science and Engineering A*. 2003;360(1-2):70-84.
- [29] Kweh SWK, Khor KA, Cheang P. An in vitro investigation of plasma sprayed hydroxyapatite (HA) coatings produced with flame-spheroidized feedstock. *Biomaterials*. 2002;23(3):775-85.
- [30] Saber-Samandari S, Berndt CC. IFTHSE Global 21: Heat treatment and surface engineering in the twenty-first century: Part 10 - Thermal spray coatings: A technology review. *International Heat Treatment and Surface Engineering*. 2010;4(1):7-13.
- [31] Tang Q, Brooks R, Rushton N, Best S. Production and characterization of HA and Si-HA coatings. *Journal of Materials Science-Materials in Medicine*. 2010;21(1):173-81.
- [32] Richard C, Kowandy C, Landoulsi J, Geetha M, Ramasawmy H. Corrosion and wear behavior of thermally sprayed nano ceramic coatings on commercially pure Titanium and Ti-13Nb-13Zr substrates. *International Journal of Refractory Metals and Hard Materials*. 2010;28(1):115-23.
- [33] Sanpo N, Tan ML, Cheang P, Khor KA. Antibacterial property of cold-sprayed HA-Ag/PEEK coating. *Journal of Thermal Spray Technology*. 2009;18(1):10-5.
- [34] Goswami R, Jana T, Ray S. Transparent polymer and diamond-like hydrogenated amorphous carbon thin films by PECVD technique. *Journal of Physics D: Applied Physics*. 2008;41(15).
- [35] Rossnagel S. Sputtering and Sputter Deposition. In: Seshan K, (ed.). *Handbook of Thin-Film Deposition Processes and Techniques - Principles, Methods, Equipment and Applications*. California: William Andrew Publishing; 2002.
- [36] Liu XY, Chu PK, Ding CX. Surface modification of titanium, titanium alloys, and related materials for biomedical applications. *Materials Science & Engineering R-Reports*. 2004;47(3-4):49-121.

- [37] Ivanova E, Wang J, Truong V, Kemp A, Berndt C, Crawford R. Bacterial Attachment onto the Surfaces of Sputter-prepared Titanium and Titanium-based Nanocoatings. In: Zacharie B. and Jerome T, (ed.) *Advances in Nanotechnology*: Nova Science Publisher; 2011.
- [38] MacMillan I. Advances in sputtering benefit coating costs. *Laser Focus World*. 2009;45(4):41-4.
- [39] Brohede U, Zhao S, Lindberg F, Mihranyan A, Forsgren J, Strømme M, et al. A novel graded bioactive high adhesion implant coating. *Applied Surface Science*. 2009;255(17):7723-8.
- [40] Wan T, Aoki H, Hikawa J, Lee JH. RF-magnetron sputtering technique for producing hydroxyapatite coating film on various substrates. *Bio-Medical Materials and Engineering*. 2007;17(5):291-7.
- [41] Pichugin VF, Surmenev RA, Shesterikov EV, Ryabtseva MA, Eshenko EV, Tverdokhlebov SI, et al. The preparation of calcium phosphate coatings on titanium and nickel-titanium by rf-magnetron-sputtered deposition: Composition, structure and micromechanical properties. *Surface and Coatings Technology*. 2008;202(16):3913-20.
- [42] Molagic A. Structural characterization of TiN/HAp and ZrO<sub>2</sub>/HAp thin films deposited onto Ti-6Al-4V alloy by magnetron sputtering. *UPB Scientific Bulletin, Series B: Chemistry and Materials Science*. 2010;72(1):187-94.
- [43] Hong Z, Mello A, Yoshida T, Luan L, Stern PH, Rossi A, et al. Osteoblast proliferation on hydroxyapatite coated substrates prepared by right angle magnetron sputtering. *Journal of Biomedical Materials Research - Part A*. 2010;93(3):878-85.
- [44] Ding SJ. Properties and immersion behavior of magnetron-sputtered multi-layered hydroxyapatite/titanium composite coatings. *Biomaterials*. 2003;24(23):4233-8.
- [45] Thian ES, Huang J, Best SM, Barber ZH, Bonfield W. A new way of incorporating silicon in hydroxyapatite (Si-HA) as thin films. *Journal of Materials Science-Materials in Medicine*. 2005;16(5):411-5.
- [46] Cooley DR, Vandellen AF, Burgess JO, Windeler AS. The advantages of coated titanium implants prepared by radiofrequency sputtering from hydroxyapatite. *Journal of Prosthetic Dentistry*. 1992;67(1):93-100.
- [47] Ievlev VM, Domashevskaya EP, Putlyayev VI, Tret'yakov YD, Barinov SM, Belonogov EK, et al. Structure, elemental composition, and mechanical properties of films prepared by radio-frequency magnetron sputtering of hydroxyapatite. *Glass Physics and Chemistry*. 2008;34(5):608-16.
- [48] Nieh TG, Jankowski AF, Koike J. Processing and characterization of hydroxyapatite coatings on titanium produced by magnetron sputtering. *Journal of Materials Research*. 2001;16(11):3238-45.

- [49] Ozeki K, Yuhta T, Fukui Y, Aoki H, Nishimura I. A functionally graded titanium/hydroxyapatite film obtained by sputtering. *Journal of Materials Science-Materials in Medicine*. 2002;13(3):253-8.
- [50] Snyders R, Bousser E, Music D, Jensen J, Hocquet S, Schneider JM. Influence of the chemical composition on the phase constitution and the elastic properties of RF-sputtered hydroxyapatite coatings. *Plasma Processes and Polymers*. 2008;5(2):168-74.
- [51] Socol G, Macovei AM, Miroiu F, Stefan N, Duta L, Dorcioman G, et al. Hydroxyapatite thin films synthesized by pulsed laser deposition and magnetron sputtering on PMMA substrates for medical applications. *Materials Science and Engineering B: Solid-State Materials for Advanced Technology*. 2010;169(1-3):159-68.
- [52] Chen W, Liu Y, Courtney HS, Bettenga M, Agrawal CM, Bumgardner JD, et al. In vitro anti-bacterial and biological properties of magnetron co-sputtered silver-containing hydroxyapatite coating. *Biomaterials*. 2006;27(32):5512-7.
- [53] Morinaga M, Yukawa H. Alloy design with the aid of molecular orbital method. *Bulletin of Materials Science*. 1997;20(6):805-15.
- [54] Abdel-Hady M, Hinoshita K, Morinaga M. General approach to phase stability and elastic properties of  $\beta$ -type Ti-alloys using electronic parameters. *Scripta Materialia*. 2006;55(5):477-80.